

# Algorithm Theoretical Basis Document for Reference Evapotranspiration (DMETREF)

**PRODUCTS: LSA-303 (DMETREF)**

The EUMETSAT  
Network of  
Satellite Application  
Facilities



**LSA SAF**

Land Surface Analysis

Reference Number: SAF/LAND/IPMA/ATBD\_METREF/1.1

Issue/Revision Index: Issue 1

Last Change: 06/07/2016

## DOCUMENT SIGNATURE TABLE

	Name	Date	Signature
<b>Prepared by :</b>	I. Trigo, H. de Bruin; in situ data provided by F. Bosveld.		
<b>Approved by :</b>	Land SAF Project Manager (IPMA)		

## DOCUMENTATION CHANGE RECORD

Issue / Revision	Date	Description:
Version 1.0	29/04/2016	ETO algorithm for SEVIRI/MSG
Version 1.1	06/07/2016	Document changes following recommendations of PCR reviewers.

## DISTRIBUTION LIST

Internal Consortium Distribution		
Organisation	Name	No. Copies
IPMA	Isabel Trigo	
IPMA	Sandra Coelho e Freitas	
IPMA	Carla Barroso	
IPMA	Isabel Monteiro	
IPMA	João Paulo Martins	
IPMA	Pedro Diegues	
IPMA	Ana Veloso	
IPMA	Pedro Ferreira	
IDL	Carlos da Camara	
IDL	Teresa Calado	
KIT	Folke-S. Olesen	
KIT	Frank Goettsche	
MF	Jean-Louis Roujean	
MF	Gregoire Jacob	
MF	Dominique Carrer	
RMI	Françoise Meulenberghs	
RMI	Arboleda Alirio	
RMI	Nicolas Ghilain	
UV	Joaquin Melia	
UV	F. Javier García Haro	
UV/EOLAB	Fernando Camacho	
UV	Aleixander Verger	

External Distribution		
Organisation	Name	No. Copies
EUMETSAT	Frédéric Gasiglia	
EUMETSAT	Dominique Faucher	
EUMETSAT	Lorenzo Sarlo	
EUMETSAT	Lothar Schueller	
EDISOFT	Tiago Sepúlveda	
EDISOFT	Joana Rosa	
EDISOFT	Joaquim Araújo	
GMV	Mauro Lima	

<b>Steering Group Distribution</b>		
<b>Nominated by:</b>	<b>Name</b>	<b>No. Copies</b>
IPMA	Pedro Viterbo	
EUMETSAT	Lothar Schueller	
EUMETSAT	Christopher Hanson	
EUMETSAT	Harald Rothfuss	
STG/AFG	Francesco Zauli	
MF	Jean-François Mahfouf	
RMI	Rafiq Hamdi	
KIT	Johannes Orphal	
VITO	Bart Deronde	

## Table of Contents

DOCUMENT SIGNATURE TABLE .....	2
DOCUMENTATION CHANGE RECORD .....	2
1 Introduction.....	7
2 Algorithm Overview .....	9
3 Algorithm Description .....	9
3.1 Theoretical Description: The Schmidt (1915) thermodynamic model ...	9
3.2 The LSA SAF Reference Evapotranspiration Algorithm .....	11
3.2.1 Error Budget Analysis.....	12
3.3 Calibration and Verification: Cabauw as a Test Case.....	12
3.3.1 In situ Data .....	13
3.3.2 Experimental Verification of the Algorithm.....	14
3.4 Practical Implementation: ETO from SEVIRI/Meteosat estimates of Solar Radiation at the Surface .....	17
3.4.1 Exception Handling .....	18
3.4.2 Examples .....	18
4 Assumptions and Limitations .....	19
4.1 Advection Effects .....	19
5 References.....	21

## List of Figures

Figure 1 Processing chain for Reference Evapotranspiration product in the LSA SAF.....	9
Figure 2 Cabauw site: eddy flux tower and surrounding landscape. ....	13
Figure 3 - Measured albedo at Cabauw for Day-of-year 90 to 275. The observations were taken over the 2007-2012 period.....	14
Figure 4 Term $\beta$ ( $Wm^{-2}$ ) from in situ observations at Cabauw obtained for the 2007-2012 period.....	15
Figure 5 Net Radiation estimated using the Slob-deBruin formulation, i.e., Equation (5) fed with in situ measurements taken at Cabauw (y-axis) versus net radiation observations. The mean difference (bias) and standard deviation are also indicated. ....	16
Figure 6 Estimates of actual evapotranspiration from eddy flux tower measurements at Cabauw (x-axis) versus ETO estimates using Equation (7) with (left) in situ observations and (right) LSA SAF DIDSSF product derived from SEVIRI/Meteosat observations. The latter are available for 2010 onwards. Average and standard deviation of the differences are also shown. ....	16
Figure 7 As in Figure 6, but using PT (Equation 8) with SdB to estimate ETO using: (left) in situ observations; and (right) LSA SAF DIDSSF product derived from SEVIRI/Meteosat observations. The latter are available for 2010 onwards. Average and standard deviation of the differences are also shown.....	17
Figure 8 Example of the LSA SAF ETO product (DMETREF in mm/day) for the 20 <sup>th</sup> January 2016 and respective number of missing slots. The latter is zoomed over South America, where there are some pixels with more than 1 missing data.....	19

## 1 Introduction

The EUMETSAT Satellite Application Facility on Land Surface Analysis (Land-SAF) is dedicated to the retrieval of information on land surfaces from remote sensing data, with emphasis on EUMETSAT satellites. The Land-SAF provides near-real-time and offline products and user support for a wide range of land surface variables related with: (i) surface radiation, both long- and short-wave components; (ii) vegetation, including state, stress and wild fires; and (iii) the energy budget at the surface, combining information on the radiation budget and vegetation state. The document presents the algorithm used by the Land-SAF for the estimation of *Reference Evapotranspiration*, Land-SAF product LSA-303, from SEVIRI/Meteosat observations.

*Reference evapotranspiration*, denoted here as  $ET_0$ , is the evapotranspiration rate from a clearly defined reference surface. The concept was introduced to allow the estimation of the evaporative demand of the atmosphere independently of crop type, crop development or management practices.

The Food and Agricultural Organization of the United Nations (FAO) published a number of reports (Doorenbos and Pruitt, 1975 and Allen et al., 1998) with guidelines for optimum water management. This ATBD will refer to the concepts and approaches defined in FAO "Irrigation and drainage paper 56" by Allen et al. (1998), hereafter denoted as FAO56. The first step in the FAO methodology is the calculation of the so-called reference (crop) evapotranspiration, denoted by  $ET_0$ . It corresponds to the evapotranspiration that a hypothetical extensive field covered with (0.12 m height) green grass with specified albedo, roughness length for heat and momentum and surface resistance, would experience under the given atmospheric conditions. It is assumed that  $ET_0$  depends on the prevailing weather conditions only, and therefore provides a characterization of the "evaporative power of the atmosphere". The water requirements of a particular crop,  $E_c$ , within a given stage in the growing season, and under the same atmospheric conditions, are assumed to be linearly related with  $ET_0$  via a crop coefficient:

$$E_c = K_c ET_0 \quad (1)$$

According to the FAO56 report, this crop evapotranspiration under standard conditions ( $E_c$ ) refers to the evaporating demand from crops - including both soil evaporation and plant transpiration - that are grown in large fields under optimum soil water, excellent management and environmental conditions, and achieve full production under the given climatic conditions. The crop coefficients are tabulated values (e.g., Allen et al., 1998), depending on the crop type and growing stage.  $E_c$  would then correspond to the expected evapotranspiration of crop  $c$ , assuming disease-free plants and optimum soil conditions.

The FAO definition of  $ET_0$  for an extensive well-irrigated grass field and its evaluation through the Penman-Monteith equation, which is derived for idealized horizontally homogeneous and uniform flat terrain, leads to an ambiguity (Garatuza-

Payan et al., 1998; McMahon et al. 2013; Katerji and Rana 2011, 2013). In practice, irrigation is most relevant in semi-arid regions where such idealized fields do not exist. Usually, weather stations concern fields smaller than 104 m<sup>2</sup> and are often surrounded by dry terrain. Under such conditions, processes that can be denoted with the generic name advection, will lead to significant inconsistencies between idealized  $ET_0$  and  $ET_0$  estimates using ground data.

Another, more fundamental drawback of the  $ET_0$  concept is that it concerns a purely hypothetical grass surface that does not exist in reality, by which experimental validation of any estimation formula for  $ET_0$  is not really possible. Note that in Allen et al (1998) there is no chapter dealing with experimental validation of the recommended methodology to calculate  $ET_0$ , being a version of the Penman-Monteith equation (hereafter PMFAO). Nonetheless, PMFAO is widely used even far outside the goals for which it is developed. The, experimental validations of PMFAO we could find in literature, concern mainly lysimeter studies in semi-arid regions installed in small fields. But, then, local advection cannot be ignored, which contradicts with the definition of  $ET_0$  that refers to extensive grass, and therefore suggesting that local advection should be ignored. This has created an ambiguous situation. Moreover, the drawback of the fact that in hydrology and hydrometeorology PMFAO is generally accepted as "the best" approach to estimate  $ET_0$ , interest in the physical background has faded. In the last decade, PMFAO has been applied, without further discussions about its validity, outside the field of irrigation, such as in climate change studies in which long term weather records gathered under non-reference conditions are analyzed. We conclude that there is a need to pay attention to actual evapotranspiration of an actual grass field that closely resembles the FAO reference surface.

With this in mind, this document presents a model to estimate  $ET_0$  using, as primary input, daily short-wave radiation at the surface derived from SEVIRI/MSG by the LSA SAF (DIDSSF, LSA-203). The algorithm is based on fundamental physical principles, applied to actual ET of a grass surface, as close to the FAO reference surface as possible. The derivation, detailed in de Bruin et al. (2016), is based on the thermodynamic model by Schmidt (1915) combined with a model for the atmospheric boundary layer. The latter has been used and tested by McNaughton and Spriggs (1986), Jacobs and de Bruin (1992) and, more recently, by Van Heerwaarden et al. (2010).

It is shown that net radiation over a FAO-like reference surface may be inferred from incoming solar radiation at the surface. Here we will use a simple empirical formulation, denoted hereafter Slob - de Bruin (de Bruin, 1987; de Bruin and Stricker, 2000, de Bruin et al., 2016). The Daily Downward Surface Shortwave Flux (DIDSSF) product generated by the LSA SAF is used from SEVIRI/MSG (Geiger et al, 2008; Trigo et al., 2011) is used to estimate net radiation over the reference surface, which in turn is the main driver of the LSA SAF  $ET_0$  product (DMETREF, LSA-303). On one hand, installation and maintenance of a ground-based network of standard meteorological (FAO) stations is increasingly expensive and labour intensive and, on the other, the availability of remote sensing data covering wide areas with high spatial and temporal samplings is increasing. This further supports the use of geostationary satellite data to derive  $ET_0$ , in line with previous studies supporting the use of remote sensing

observations for the estimation of crop reference evapotranspiration (e.g., Choudhury and de Bruin, 1995; Bois et al., 2008; Hart et al., 2009; de Bruin et al., 2010, 2012; Cammalleri and Ciraolo, 2013).

## 2 Algorithm Overview

The LSA SAF  $ET_0$  product (DMETREF, LSA-303) is estimated from daily estimations of Downward Surface Shortwave Flux (DIDSSF) product generated by the LSA SAF from SEVIRI/Meteosat. As detailed in the sections below, it is shown that  $ET_0$  can be computed from the daily net radiation and since  $ET_0$  refers to a well-known and well-watered reference surface, daily net radiation over such surface is essentially driven by short-wave radiation. Therefore, daily short-wave radiation at the surface estimated from SEVIRI, i.e., DIDSSF (LSA-203) product is the main input for DMETREF (LSA-303), as shown in Figure 1. The algorithm and product characteristics of DIDSSF are described in the respective LSA SAF documents (LSA SAF DSSF ATBD and LSA SAF DSSF PUM, both available at the LSA SAF website <http://landsaf.ipma.pt>).

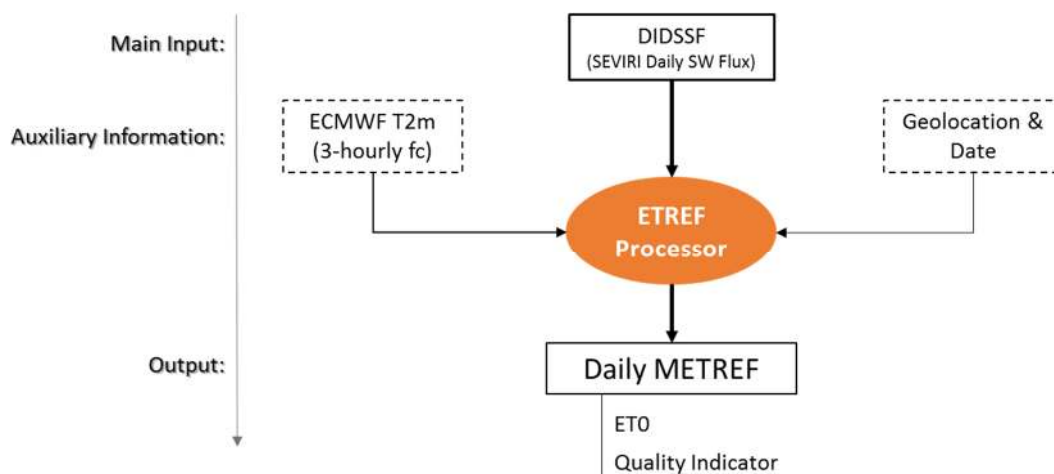


Figure 1 Processing chain for Reference Evapotranspiration product in the LSA SAF.

## 3 Algorithm Description

### 3.1 Theoretical Description: The Schmidt (1915) thermodynamic model

The rationale for the  $ET_0$  algorithm has been published by de Bruin and Holtslag (1982; their formula 10), who referred to arguments used by Schmidt (1915) to estimate the evaporation of ocean surface, reformulated for a non-stress and extensive grass surface as recently explained by de Bruin et al (2016). We consider a hypothetical flat box at the grass surface, encompassing the vegetated surface, a soil layer, and the

lowest layer of the atmosphere with height  $h$ . So, the volume of the box equals  $hO$ , where  $O$  is the area of the bottom of the box. Since we consider well-watered grass surface, we assumed that water vapour in the box is saturated at surface temperature. Next we consider a thermodynamic process in which during a short period of time,  $dt$ , an amount of energy  $dQ$  is added, which corresponds to an available energy flux density  $A$  (in  $\text{Wm}^{-2}$ ). As a result the temperature in the box will increase by  $dT$  and a part of the added energy is used to increase the enthalpy of the air in the box by  $m_a c_p dT$ , where  $m_a$  is the mass of air in the box and  $c_p$  the specific heat of air at constant pressure. Obviously,  $m_a = \rho h O$  and, taking into account the equation of state for air, this can be written as  $m_a = (p/RT)hO$  with  $p$  being the air pressure and  $R$  the specific gas constant of air. By dividing the increase of enthalpy in the box by  $Odt$ , the mean sensible heat flux density  $H = (p/RT)c_p h dT/dt$  is obtained. Assuming, as Schmidt did, that the air in the box remains saturated, the water vapor pressure in the box will increase by  $e_s(T + dT) - e_s(T) \approx \Delta dT$ , with  $e_s(T)$  being the saturated water vapour pressure at temperature  $T$  and  $\Delta = de_s/dT$ , also at  $T$ . As a result, the mass of water vapor will increase by  $dm_v$ . With the equation of state for water vapour we find that  $dm_v = (\Delta dT/R_v T)hO$ . The energy required to evaporate this amount of water is  $\lambda dm_v$ . By dividing by  $Odt$  we obtain the latent flux density  $= \frac{\lambda \Delta}{(R_v T)} h dT/dt$ . With  $\gamma = (R_v/R)(c_p p/\lambda)$  (Annex 1), we find that the ratio  $B$  of the increase of the enthalpy of the air in the box and the energy required for evaporation to keep the water vapour pressure saturated is given by:

$$B = \frac{\gamma}{\Delta} \quad (2)$$

Note that  $B$  can be identified as the Bowen ratio  $B = H/\lambda ET$ , and that  $A = H + \lambda ET$ . This result is obtained for a time step  $dt$ . As an extension of Schmidt's approach, we introduce a hypothetical valve in the top of the box, so that at the end of time step  $dt$  the increase of enthalpy and water vapour formed in the box during  $dt$  can be released into the atmosphere. It is assumed that no energy is required for this release. At the end of each time step the temperature and water vapour content will be reset at their initial values. In the next time interval  $dt$  the process is repeated. For a number of time steps this is repeated covering a total of about 10-minutes. In the next 10-minute period we start with the new actual surface temperature. In this way a quasi-stationary process is simulated for the vertical transfer of heat and water vapour from the surface into the atmosphere. In our case  $A = Q^* - G$ , where  $Q^*$  is the net radiation and  $G$  is the amount of heat stored in the vegetation-soil part in the box. Because we consider 24-hourly averages,  $G$  can be ignored. In this way, we arrive at:

$$\lambda ET = \frac{\Delta}{\Delta + \gamma} Q^* \quad (3)$$

The only assumption made so far is that air over well-watered surfaces close to the ground is saturated. With Schmidt (1915), we recognize that in real life this is not true and that corrections should be made. Following de Bruin and Holtslag (1982) the correction consists of adding a constant  $\beta$ , which leads to :

$$\lambda ET = \lambda ET_{eq} + \beta \quad (\text{W m}^{-2}) \quad (4)$$

Note that (Beljaars and Bosveld 1997) confirmed these findings analysing an independent dataset gathered later at Cabauw. A physical explanation is the entrainment of relatively warm and dry air present aloft the atmospheric boundary layer (ABL) into the well-mixed ABL during daytime. Consequently, relative humidity in the ABL is less than 100%, despite the high surface evaporation rate. This explains why a correction factor should be used. The introduction of the constant  $\beta$  will be discussed later.

It is worth pointing that Eq (3) can also be interpreted as a particular case of the Penman-Monteith equation (see e.g., FAO56) considering a saturated surface (with canopy resistance  $r_s = 0$ ) and that the air above it is also saturated (with water vapour pressure deficit  $\delta e = 0$ ). As recognised above, the introduction of the constant  $\beta$  aims to correct for deviations of the underlying assumptions with respect to reality.

Next we describe how daily net radiation over a well-watered grass surface can be determined from daily solar radiation.

### 3.2 The LSA SAF Reference Evapotranspiration Algorithm

It is important to note that in eq. (3)  $Q^*$  is the net radiation of the hypothetical well-watered reference grass surface. "Surface dryness" will affect the actual net radiation. When the surface is dry the surface temperature will be relative high compared to reference conditions. De Bruin (1987) reported this feature for grass in the Netherlands in the very dry year of 1976 and the normal year 1977 when water stress could be ignored. He reported that net radiation for well-watered grass can be estimated by using the so-called Slob-de Bruin formula (hereafter SdB):

$$Q_r^* = (1 - 0.23)K^\downarrow - C_S \frac{K^\downarrow}{K_{ext}^\downarrow} \quad (5)$$

where  $Q_r^*$  is the net radiation over the grass reference surface with an albedo of 0.23,  $K^\downarrow$  is the down-welling short-wave radiation at the surface (LSA SAF product DIDSSF),  $K_{ext}^\downarrow$  is the down-welling short-wave radiation constant at the top of the atmosphere (Annex 2), and  $C_S$  an empirical constant. De Bruin (1987) reported for unstressed grass of Cabauw  $C_S = 110 \text{ W m}^{-2}$ . The "universality" of SdB will be discussed later.

This yields:

$$\lambda ET_0 = \frac{\Delta}{\Delta + \gamma} \left[ (1 - 0.23)K^\downarrow - C_S \frac{K^\downarrow}{K_{ext}^\downarrow} \right] + \beta \quad (6)$$

and therefore:

$$ET_0 = \frac{1}{\lambda} \left( \frac{\Delta}{\Delta + \gamma} \left[ (1 - 0.23)K^\downarrow - C_S \frac{K^\downarrow}{K_{ext}^\downarrow} \right] + \beta \right) \quad (7)$$

Evapotranspiration over the reference surface can be inferred through the application of Eq. (8) to estimations of obtained from remote sensing data, such as MSG.

The set of Eqs (3) and (4), and therefore (6) and (7) are very close to the Priestley-Taylor equation (PT, Priestley and Taylor, 1972):

$$ET_{0PT} = \alpha \frac{1}{\lambda} \frac{\Delta}{\Delta + \gamma} (Q_r^* - G) \quad (8)$$

where  $\alpha$  is a dimensionless constant and  $G$  is the ground flux, which we can also assume to be negligible over a full day. Priestley and Taylor (1972) proposed  $\alpha=1.26$  for “advection-free” saturated surfaces, as is the case of the reference surface considered here. The PT has been widely used for the estimation of reference evapotranspiration (e.g., McMahon et al., 2013). Here we will compare the outcome of the PT method, assuming  $G=0$  and  $Q_r^*$  given by the SdB formulation (eq. 5).

### 3.2.1 Error Budget Analysis

We consider that reference evapotranspiration provided by Eq. (7) has two main sources of error, namely: (i) propagation of  $K^\downarrow$  uncertainties, i.e., propagation of errors in the estimation of DIDSSF LSA SAF product; and (ii) uncertainties in the parameterizations used in equation (7), i.e. associated to the overall assumptions that actual evapotranspiration over an extensive surface covered by well-watered grass ( $ET_0$ ) may be determined from incoming daily solar radiation if parameters  $\beta$  and  $C_s$  are known. Considering the above sources of uncertainty are independent, the variance of the estimates error is given by:

$$S_{ET_{K^\downarrow}}^2 = \left( \frac{1}{\lambda} \frac{\Delta}{\Delta + \gamma} \left[ (1 - 0.23) - C_s \frac{1}{K_{ext}^\downarrow} \right] \right)^2 S_{K^\downarrow}^2 + S_{Alg}^2 \quad (9)$$

where  $S_{K^\downarrow}^2$  is the variance of  $K^\downarrow$  error and  $S_{Alg}^2$  is the variance of the parameterization errors; the latter is assumed the inputs are error free.

### 3.3 Calibration and Verification: Cabauw as a Test Case

The method described in the previous section has been verified using in situ measurement of radiation (solar and net) and of actual evapotranspiration measured over a surface resembling the reference one used in  $ET_0$  definition. For this purpose, we have used data gathered at the experimental grass site, managed by KNMI since 1972, and described in de Bruin and Holtslag (1982) and (Beljaars and Bosveld 1997), later named as the Cabauw Experimental Site for Atmospheric Research (CESAR).

Cabauw is located in the western part of The Netherlands (51.971°N, 4.927°E), within the mid-latitude climate zone where droughts are rare. The site and surrounding area are dominated by non-irrigated grass (Figure 2). The soil consists of a 0.7-m thick clay layer on top of a thick peat layer. The ground water table is managed by a dense network of ditches, and only rarely droughts have reduced evapotranspiration. The terrain around the site also corresponds to grassland, which was free from obstacles up

to a few hundred meters in all directions during the whole study period considered in this document (2010-2012). For further details about CESAR observatory see Monna and Bosveld (2013). Given its geographical location and local characteristics, the Cabauw test area resembles closely the hypothetical FAO reference grass for conditions without advection. The wide range of available local observations together with site characteristics make this a unique test base for studies of reference evapotranspiration: as discussed in de Bruin et al (2016), this is one of the rare cases where actual evapotranspiration over a large area actually corresponds to Reference Evapotranspiration, as defined by FAO56.



**Figure 2 Cabauw site: eddy flux tower and surrounding landscape.**

### 3.3.1 In situ Data

We consider the so-called validated and gap-filled meteorological surface data and surface flux files (<http://www.cesar-database.nl/>), for the 2010-2012 period. This concerns 10-minute values from which obtained from the energy budget residual method (Beljaars and Bosveld 1997).

The database includes a net radiometer data as well as separate observations of the four components of net radiation, i.e. incoming and reflected short-wave radiation (denoted here  $K^\downarrow$  and  $K^\uparrow$ , respectively) and incoming and outgoing longwave radiation, here denoted with  $L^\downarrow$  and  $L^\uparrow$ . We excluded days for which directly measured net radiation differs more than  $15 \text{ Wm}^{-2}$  from that calculated using the 4 components.

The albedo obtained from  $K^\downarrow$  and  $K^\uparrow$  measured at Cabauw is shown in Figure 3. It is seen that the albedo varies from day to day but on average its value is very close to 0.23, i.e. the value of the reference grass surface defined by Allen et al., (1998). Considering the environmental conditions of the Cabauw site regarding e.g. albedo, water stress, advection, we are confident to state that the Cabauw site resembles fairly close the hypothetical idealized reference grass surface.

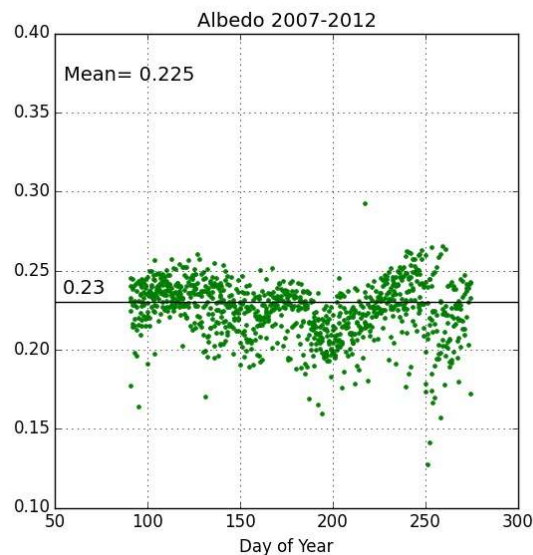


**Figure 3 - Measured albedo at Cabauw for Day-of-year 90 to 275. The observations were taken over the 2007-2012 period.**

### 3.3.2 Experimental Verification of the Algorithm

#### (i) The $\beta$ -parameter

Bruin and Holstag (1982) considered some empirical features of hourly values of  $\beta$  during day-time. Since we consider here 24-hourly averages we show here Figure 4 depicting empirical estimations of the term  $\beta$  in Equation (7), i.e., the residual from in situ (actual) ET obtained from eddy-flux measurements minus the estimates using Equation (3) with in situ net radiation observations at Cabauw as described by de Bruin et al. (2016). It is seen that, strictly speaking,  $\beta$  is not constant indeed, but the random scatter around its mean value of about  $20 \text{ W m}^{-2}$  is relatively small: the 2007-2012 data at Cabauw gives an averaged value for  $\beta$  of  $17 \text{ W m}^{-2}$  and a standard deviation of  $7.6 \text{ W m}^{-2}$ . This scatter results in a random error in  $ET_0$  of  $0.26 \text{ mm/day}$ . The deviation of the average from value originally estimated by de Bruin and Holstag (1982) corresponds to an error in  $ET_0$  of about  $0.1 \text{ mm/day}$ . The data at Cabauw suggests therefore the contribution of the uncertainty the term  $\beta$  to the total uncertainty associated to the algorithm,  $S_{Alg}$  (Equation 9) of the order of  $0.3 \text{ mm/day}$ .

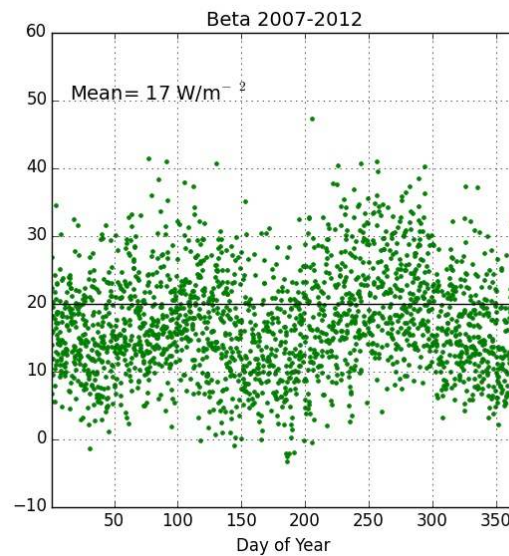


**Figure 4** Term  $\beta$  ( $\text{Wm}^{-2}$ ) from in situ observations at Cabauw obtained for the 2007-2012 period.

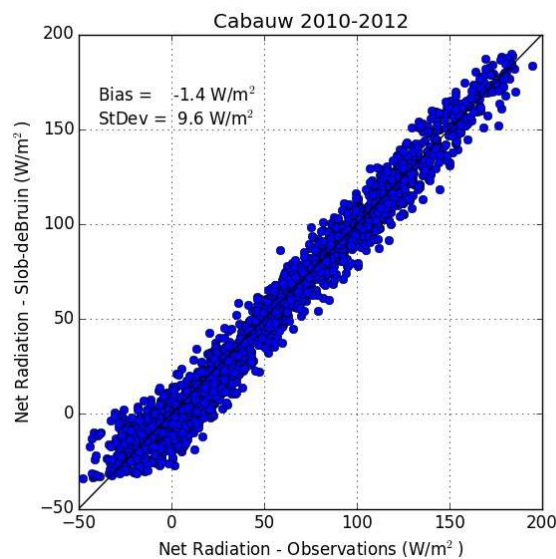
(ii) The Slob-DeBruin formulation for net radiation

Figure 5 shows a test of the Slob-deBruin method (Equation 5) to estimate net radiation in Cabauw. The results show a very good agreement between Slob-deBruin estimates and local observations, with an average difference of  $-1.4 \text{ Wm}^{-2}$  and a standard deviation of the differences below  $10 \text{ Wm}^{-2}$  (Figure 5). Assuming that Cabauw may be used as a test site for the reference FAO surface, this yields a contribution to the total uncertainty in the estimation of  $ET_0$  using equation (7) of less than  $0.23 \text{ mm/day}$ .

(iii) Algorithm uncertainty

The conditions at Cabauw allow the use of local measurements to make an estimate of the total uncertainty associated to the algorithm described above, which led to Equation (7). In this case we assume the input data is error free and we are only accounting for uncertainties in the parameterizations. The data described in the points above suggests that  $0.3 \text{ mm/day}$  is an acceptable estimate for the assumption that parameter  $\beta$  is constant, while  $0.23 \text{ mm/day}$  is acceptable as an uncertainty estimate associated to the estimate of daily net radiation from daily estimate of the short-wave component through Equation (5). As such, the uncertainty of the algorithm,  $S_{Alg}$  may be assumed to be less than  $0.4 \text{ mm/day}$ .

This result is consistent with the validation of Equation (7) using as input data in situ observations gathered in Cabauw show in Figure 6. For the 2007-2012 period, these reveal an average and standard deviation of differences of  $-0.1 \text{ mm/day}$  and  $0.3 \text{ mm/day}$ , respectively. The results do not change significantly when Equation (7) is applied to LSA SAF DIDSSF product (only available from 2010 onwards) with a bias  $+0.1 \text{ mm/day}$  and standard deviation of differences of  $0.3 \text{ mm/day}$ .



**Figure 5 Net Radiation estimated using the Slob-deBruin formulation, i.e., Equation (5) fed with in situ measurements taken at Cabauw (y-axis) versus net radiation observations. The mean difference (bias) and standard deviation are also indicated.**

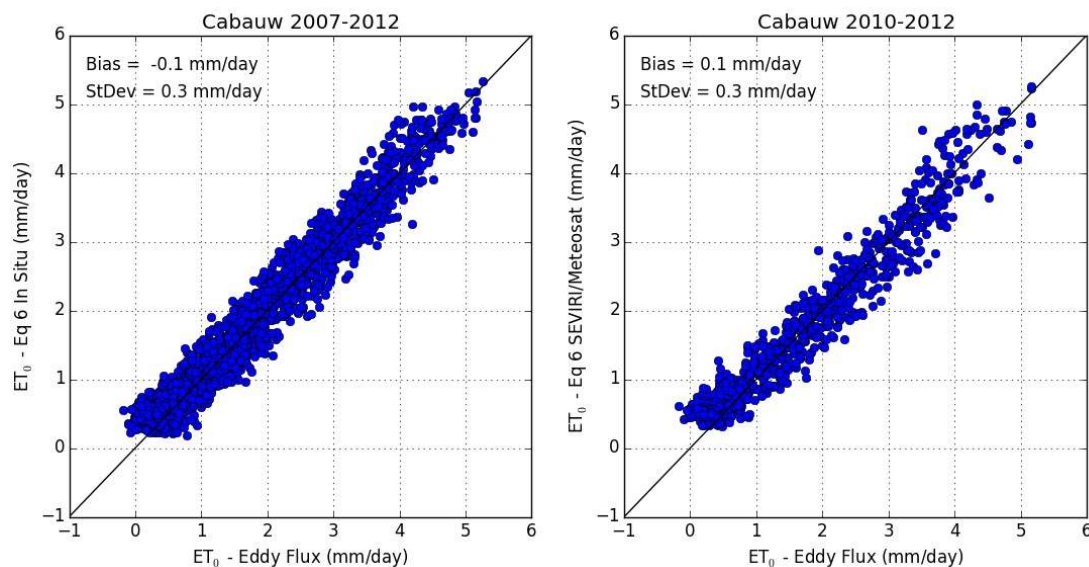


**Figure 6 Estimates of actual evapotranspiration from eddy flux tower measurements at Cabauw (x-axis) versus ET<sub>0</sub> estimates using Equation (7) with (left) in situ observations and (right) LSA SAF DIDSSF product derived from SEVIRI/Meteosat observations. The latter are available for 2010 onwards. Average and standard deviation of the differences are also shown.**

One of the main advantages of the method proposed here based on Equation (7) is its simplicity, allowing the estimation of ET<sub>0</sub> from remote sensing products, such as incoming solar radiation. The same argument could be, however, applied to the Priestley-Taylor equation (Priestley and Taylor, 1972), which has long been applied as

an alternative for the derivation of  $ET_0$ . For completeness, we have also compared PT  $ET_0$  estimates, where net radiation is computed using the SdB approach (Equation 5) with measurements gathered at Cabauw. As shown in Figure 7, the PT tends to overestimate (underestimate) higher (lower) ET values.

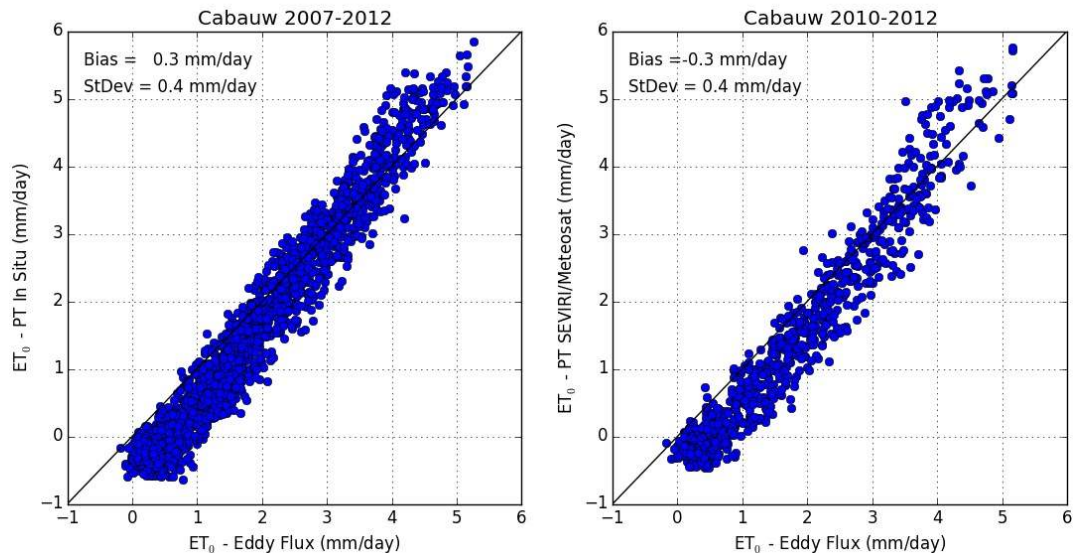


**Figure 7** As in Figure 6, but using PT (Equation 8) with SdB to estimate  $ET_0$  using: (left) in situ observations; and (right) LSA SAF DIDSSF product derived from SEVIRI/Meteosat observations. The latter are available for 2010 onwards. Average and standard deviation of the differences are also shown.

### 3.4 Practical Implementation: $ET_0$ from SEVIRI/Meteosat estimates of Solar Radiation at the Surface

The results discussed above for Cabauw suggest that Equation (7) is suitable for the estimation of actual evapotranspiration over an extensive surface of well-watered grass, i.e., for the estimation of Reference Evapotranspiration,  $ET_0$ , from daily values of solar radiation at the surface. The algorithm provides acceptable values with an acceptable uncertainty of the order of 0.4 mm/day or less. This makes the formulation given by Equation (6) a viable alternative to determine  $ET_0$  from remote sensing estimations of solar radiation fluxes at the surface, such as DIDSSF product from the LSA SAF (LSA-203).

The daily global radiation product, DIDSSF, operationally delivered by the EUMETSAT LSA SAF from SEVIRI/Meteosat has shown to meet its target accuracy of 10% under most circumstances; the threshold accuracy for the product is 20% (LSA SAF DSSF VR; Ineichen et al., 2008; Carrer et al. 2012). The exercise presented here for Cabauw sustains that DIDSSF may be used for  $ET_0$  estimation; further analysis of the capability of

DIDSSF to estimate net radiation and therefore  $ET_0$  may be found in the Validation Report of the LSA SAF METREF product.

Within the LSA SAF, daily  $ET_0$ , i.e., METREF (LSA-303), is therefore estimated from DIDSSF on a pixel-by-pixel basis. As the main input for the product, it is considered that the quality of DIDSSF will be the main factor conditioning that of METREF. In turn, the former is strongly linked to the number of instantaneous estimates of downward surface solar flux (DSSF) per day and per pixel available, which are used for integration in time (0 to 24 UTC) into DIDSSFs. The number of missing data SEVIRI/Meteosat data per pixel is suggested to be used as a quality indicator of METREF, as already used for DIDSSF.

### 3.4.1 Exception Handling

The following input data per pixel are mandatory to estimate METREF; if any is missing, METREF is set to “missing value”:

- DIDSSF and respective quality flag (number of daily observations per pixel missing);
- Air Temperature at 2m. These are obtained from ECMWF operational forecasts, interpolated to SEVIRI/MSG pixels within the LSA SAF processing chain, as part of the pre-processing package used by all LSA SAF products. The hourly values of 2m temperature are averaged over each day and used and used to estimate the thermodynamic properties required for Equation (6) and (7), as detailed in Annex 1.
- Pixel latitude and observation date required for the estimation of extra-terrestrial radiation, as detailed in Annex 2.

### 3.4.2 Examples

DMETREF is generated for all land pixels within Meteosat disk (nominal longitude at  $0^\circ$ ), for which mandatory input data is available, as shown in Figure 8. The number of missing slots for the daily integration of solar radiation is also shown. This example corresponds to the most common conditions, where the number of missing slots is very low (1 or less). There are very few cases, for which instantaneous solar fluxes at the surface cannot be estimated, as in the scattered pixels over South America in light blue Figure 8; towards the edge of the disk, this number might increase further.

Users are advised to avoid using DMETREF values where the number of missing slots is 5 or higher. DIDSSF is currently estimated from 30-min observations, i.e., out of a maximum of 48 observation per day and per pixel.

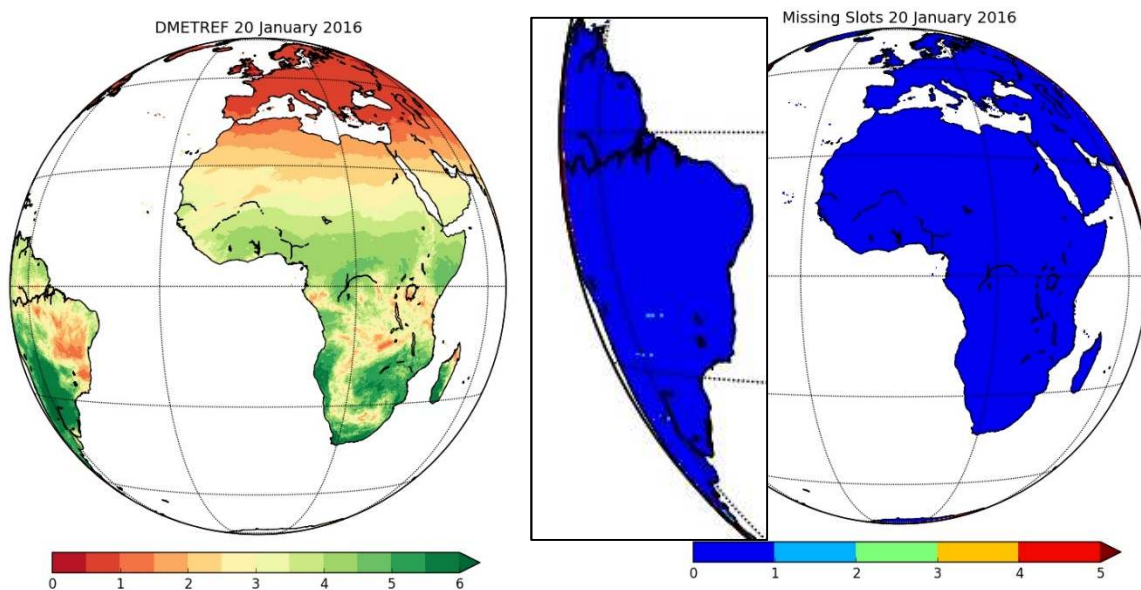


**Figure 8** Example of the LSA SAF  $ET_0$  product (DMETREF in mm/day) for the 20<sup>th</sup> January 2016 and respective number of missing slots. The latter is zoomed over South America, where there are some pixels with more than 1 missing data.

## 4 Assumptions and Limitations

The rationale for the reference evapotranspiration algorithm proposed for the LSA SAF is entirely based on a model for actual ET of actual grass that is close to hypothetical FAO grass, accepting the interpretation in the FAO definition "extensive field" excludes advection. As thoroughly discussed in de Bruin et al. (2016), the methodology is based on thermodynamic model by Schmidt (1915), published 100 years ago. Furthermore, it is argued that the air above well-watered grass is never saturated because after sunrise warm and dry air is entrained into the ABL, explaining the need for the correction factor  $\beta$  in Equation (7).

### 4.1 Advection Effects

There is an ambiguity in the FAO definition concerning effects of local advection, which makes difficult the estimation and assessment of crop reference evapotranspiration. However, if in irrigation water management the FAO-definition of  $ET_0$  is interpreted such that local advection should be excluded, then the model presented here can be applied to estimate  $ET_0$ . It should be taken into account that if local advection is to be included, then this model will lead to an underestimation of  $ET_0$ .

Advection effects may be relevant in cases where an actual well-watered grass field is embedded in a semi-arid environment. There is one such experimental field near Cordoba (Southern Spain), where a field has been designed to resemble as close as possible FAO reference grass, except that the size of the field is not 'extensive, but limited to 100 x 100 m<sup>2</sup>. In the dry season the surrounding is often dry. Berengena and

Gavilán (2005) showed that actual ET measured with a precision lysimeter in the centre of this field exceeds net radiation by the end of the dry season, and that  $ET_0$  tends to be underestimated. Under the conditions observed in Cordoba, sensible heat advected from upwind dry terrain is an additional energy source for ET. Then Schmidt's thermodynamic approach, including corrections for entrainment, leads to:

$$\lambda ET = \frac{\Delta}{\Delta + \gamma} (Q^* + Q_{adv}) + \beta \quad (10)$$

where  $Q_{adv}$  is the sensible heat horizontally advected from dry upwind terrain. Besides meteorological variables, this additional energy term will depend on the properties and dimensions of the upwind terrain. The question how to parameterize in terms of easy to measure meteorological quantities, is being investigated. In irrigation practice, often the FAO formula for crop reference evapotranspiration is applied in semi-arid regions using meteorological data gathered over small fields, by which local advection is expected to play a role. Tacitly, it is then assumed that this formula includes effects of  $Q_{adv}$  regardless the properties of adjacent fields.

The  $ET_0$  model presented in this document (de Bruin et al., 2016) can be applicable in other areas, e.g. in lumped rainfall-runoff models it can be applied to estimate the so-called potential evapotranspiration, see e.g. (Oudin et al. 2005). Furthermore, this approach can be applicable in climate change studies such as carried out by e.g. van der Schrier et al. (2006) and Sheffield et al. (2012).

## 5 References

Allen, R.G., Pereira, L.S., Raes, D., Smith, M., 1998: Crop Evapotranspiration: Guide-lines for Computing Crop Water Requirements. Irrigation and Drainage Paper No. 56. FAO, Rome, Italy, pp 300.

Beljaars, A.C.M. and F. Bosveld, 1997: Cabauw Data for the Validation of Land Surface Parameterization Schemes, *J. Climate*, 10, 1172 - 1193.

Berengena, J., Gavilán, P., 2005. Reference evapotranspiration estimation in a highly advective semiarid environment. *J. Irrig. Drain. Eng. ASCE* 131 (2), 147–163.

Bois, B., Pieria, P., Van Leeuwen, C., Wald, L., Huard, F., Gaudillere, J.-P., and Saur, E., 2007: Using remotely sensed solar radiation data for reference evapotranspiration estimation at a daily time step, *Agr. Forest. Meteorol.*, 148(4), 619–630.

Bolton, D., 1980: The computation of equivalent potential temperature, *Mon. Wea. Rev.*, 108, 1046-1053.

Cammalleri, C. and G. Ciraolo, 2013: A simple method to directly retrieve reference evapotranspiration from geostationary satellite images, *Int. J. of Appl. Earth Obs. and Geoinfo.* 21, 149–158.

Carrer, D., S. Lafont, J.-L. Roujean, J.-C. Calvet, C. Meurey, P. Le Moigne, and I. F. Trigo (2012): Incoming solar and infrared radiation derived from METEOSAT: impact on the modeled land water and energy budget over France, *J. Hydrometeorol.*, 13, 504-520. DOI: 10.1175/JHM-D-11-059.1.

Choudhury, B. J. and De Bruin, H. A. R.: First order approach for estimation unstressed transpiration from meteorological satellite data, *Adv. Space Res.*, 16(8), 167–176, 1995.

De Bruin, H.A.R., 1987: From Penman to Makkink. *Comm. Hydrol. Res.TNO, Den Haag. Proc. and Inform.*, 39, 5-30.

De Bruin, H.A.R. and A.A.M. Holtslag, 1982: A simple parameterization of the surface fluxes of sensible and latent heat during daytime compared with the Penman-Monteith concept. *J. Appl. Meteor.*, 21, 1610-1621.

De Bruin, H.A.R. and J.N.M. Stricker, 2000: 'Evaporation of grass under non-restricted soil moisture conditions'. *Hydrological Sciences*, 45, 3, 391- 406.

De Bruin, H. A. R., I. F. Trigo, F. C. Bosveld and J.F. Meirink, 2016: A thermodynamically based model for actual evapotranspiration of an extensive grass field close to FAO reference, suitable for remote sensing application, *J. Hydrometeorol.*, doi: 10.1175/JHM-D-15-0006.1

De Bruin, H.A.R., I. F. Trigo, M. A. Jitan, Temesgen Enku N., C. van der Tol and A.S.M. Gieske, 2010: Reference crop evapotranspiration derived from geo-stationary satellite imagery. A case study for the Fogera flood plain, NW-Ethiopia and the Jordan Valley, Jordan, *Hydrol. Earth Syst. Sci.*, 14, 2219–2228

De Bruin, H.A.R., I.F. Trigo, P. Galivan, A. Martinez and M.P. Gonzales, 2012 : Reference crop evapotranspiration estimated from geostationary satellite imagery, Remote Sensing and Hydrology (Proceedings of a symposium held at Jackson Hole, Wyoming, USA, September 2010), IAHS Publ. 352, 2012.

Doorenbos, J. and Pruitt, W.O. 1975. Guidelines for predicting crop water requirements, Irrigation and Drainage Paper 24, Food and Agriculture Organization of the United Nations, Rome, 179 p.

Garatuza-Payan, J., Shuttleworth, W.J., Encinas, D., Mcneil, D.D., Stewart, J.B., Bruin, H.A.R. de, and Watts, C., 1998. Measurement and modelling evaporation for irrigated crops in northwest Mexico, Hydr. Processes 12: 1397–1418.

Garratt, J. R., 1992: The atmospheric boundary layer. Cambridge University Press. 316 pp.

Geiger, B., C. Meurey, D. Lajas, L. Franchistéguy, D. Carrer, and J.-L. Roujean, 2008: Near real-time provision of downwelling shortwave radiation estimates derived from satellite observations. Meteorol. Appl. 15, pp. 411–420. DOI: 10.1002/met.84

Hart, Q., Brugnach, M., Temesgen, B., Rueda, C., Ustin, S. and Frame, K., 2009: Daily reference evapotranspiration for California using satellite imagery and weather station measurement interpolation. Civil Eng. Environ. Syst., 26, 19-33.

Ineichen, P., C. Barroso, B. Geiger, R. Hollmann, A. Marsouin, and R. Mueller, 2009: Satellite Application Facilities irradiance products: Hourly time step comparison and validation over Europe. Int. J. Remote Sens., 30, 5549–5571.

Jacobs, C. M. J. and H. A. R. De Bruin, 1992: The Sensitivity of Regional Transpiration to Land-Surface Characteristics: Significance of Feedback, J. Climate, 5, 683–698.

Katerji, N. and G. Rana 2011: Crop Reference Evapotranspiration: A Discussion of the Concept, Analysis of the Process and Validation. Water Resour Manage 25, 1581–1600.

Katerji, N. and G. Rana , 2013: FAO-56 methodology for determining water requirement of irrigated crops: critical examination of the concepts, alternative proposals and validation in Mediterranean region, Theor Appl Climatol, DOI 10.1007/s00704-013-0972-3

LSA SAF DSSF ATBD, DSSF Algorithm Theoretical Basis Document, 2012, SAF/LAND/MF/ATBD\_DSSF/1.0, <http://landsaf.ipma.pt/>

LSA SAF DSSF PUM, DSSF Product User Manual, 2011, AF/LAND/MF/PUM\_DSSF/2.6v2, <http://landsaf.ipma.pt/>

LSA SAF DSSF VR, DSSF Validation Report, 2011, SAF/LAND/MF/VR\_DSSF/I\_11v4, <http://landsaf.ipma.pt/>

McMahon, T. A., M. C. Peel, L. Lowe, R. Srikanthan, and T. R. McVicar, 2013: Estimating actual, potential, reference crop and pan evaporation using standard meteorological data: a pragmatic synthesis. Hydrol. Earth Syst. Sci., 17, 1331–1363.

McNaughton, K.G. and Spriggs, T.W., 1986. A Mixed-Layer Model for Regional Evaporation. *Boundary-Layer Meteorology*, 34(3): 243-262

Monna, Wim and Fred Bosveld, 2013: In Higher Spheres, 40 years of observations at the Cabauw Site, KNMI-Publication 232, de Bilt, 56 pp.

Oudin, L, F. Hervieu, C. Michel, C. Perrin, V. Andreassian, F. Anctil, C. Loumagne, 2005: Which potential evapotranspiration input for a lumped rainfall-runoff model? Part 2—Towards a simple and efficient potential evapotranspiration model for rainfall-runoff modelling, *Journal of Hydrology* 303 (2005) 290–306.

Priestley, C.H.B., and R.J. Taylor, 1972: On the assessment of surface heat flux and evaporation using large-scale parameters. *Mon. Weather Rev.*, 100, 81-92.

Schmidt, W., 1915: Strahlung und Verdunstung an freien Wasserflächen; ein Beitrag zum Warmehaushalt des Weltmeers und zum Wasserhaushalt der Erde (Radiation and evaporation over open water surfaces; a contribution to the heat budget of the world ocean and to the water budget of the earth). *Annalen der Hygrographie und Maritimen Meteorologie* 43, 111-124, 169-178.

Sheffield, J., E. F. Wood, and M. L. Roderick, 2012: Little change in global drought over the past 60 years, *Nature*, 491(7424), 435–438, doi:10.1038/nature11575

Trigo, I. F., C. C. DaCamara, P. Viterbo, J.-L. Roujean, F. Olesen, C. Barroso, F. Camacho-de Coca, D. Carrer, S. C. Freitas, J. García-Haro, B. Geiger, F. Gellens-Meulenberghs, N. Ghilain, J. Meliá, L. Pessanha, N. Siljamo, and A. Arboleda, 2011: The Satellite Application Facility on Land Surface Analysis. *Int. J. Remote Sens.*, 32, 2725-2744, doi: 10.1080/01431161003743199

van der Schrier, G., Briffa, K. R., Jones, P. D. & Osborn, 2006: T. J. Summer moisture variability across Europe. *J. Clim.* 19, 2818-2834.

van Heerwaarden CC, Vilà-Guerau de Arellano J, Gounou A, Guichard F, Couvreur F (2010) Understanding the daily cycle of evapotranspiration: a method to quantify the influence of forcings and feedbacks. *J. Hydrometeorol* 11:1405–1422. doi:10.1175/2010JHM1272.1

## Annex 1 Thermodynamic properties of dry air and water vapour

The following basic quantities are considered for the estimation of LSA SAF DMETREF product using Equation (8):

- Mean molecular mass for dry air  $M_d$ : 28.965 kg mol<sup>-1</sup>
- Mean molecular mass for water vapour  $M_v$ : 18.015 kg mol<sup>-1</sup>
- Specific heat capacity for dry air  $c_p$ : 1005 J kg<sup>-1</sup> °C<sup>-1</sup>  
 $c_p$  has a weak dependency with temperature, which is ignored here (in temperatures range of [-30, 50°C]  $c_p$  varies from 1005.0 to 1006.6 J kg<sup>-1</sup> °C<sup>-1</sup>).
- The ratio of molecular weight of water and dry air,  $\epsilon$ : 0.622
- Latent heat of vaporization,  $\lambda$ : 2.502 x 10<sup>6</sup> J kg<sup>-1</sup> at T=0°C  
 $\lambda$  varies with temperature, although the impact on Equation (8) estimates is unnoticeable:  $\lambda \approx 2.5\ 502 \times 10^6 - 2250 \times T$  (J kg<sup>-1</sup>; T in °C).

The values above are tabulated in Garratt (1992).

The slope of the saturation water vapour pressure,  $\Delta$ , is computed assuming the following approximation of saturation water vapour pressure,  $e_{sat}(T)$ , based on Bolton (1980):

$$e_{sat}(T) = 6.112 \exp[17.67 (T)/(T + 243.5)]$$

Where T is the temperature in °C and  $e_{sat}(T)$  is in hPa. We then have (in hPa/°C):

$$\Delta = \frac{17.67}{T + 243.5} \left( 1 - \frac{T}{T + 243.5} \right) e_{sat}(T)$$

The temperature  $T$  is obtained from ECMWF operational hourly forecasts of – meter air temperature, interpolated in space and time to SEVIRI/MSG pixels. These are then averaged over each day (0-24 UTC) to yield the variable  $T$  used in the equations described here.

The psychrometric constant,  $\gamma$  (hPa/°C<sup>-1</sup>), is given by:

$$\gamma = \frac{c_p P_{sfc}}{\epsilon \lambda}$$

Where  $P_{sfc}$  is the surface air pressure (hPa).

$P_{sfc}$  may be obtained from ECMWF forecasts, following the procedure described for  $T$ . The first version of the DMETREF implemented used a constant value of 1005 hPa for surface pressure.

## Annex 2 Extraterrestrial Radiation

Extra-terrestrial radiation, or the down-welling short-wave radiation at the top of the atmosphere,  $K_{ext}^{\downarrow}$  is given by:

$$K_{ext}^{\downarrow} = \frac{S}{\pi d_r^2} (\omega \sin(\varphi) \sin(\delta) + \cos(\varphi) \cos(\delta) \sin(\omega))$$

Where

$S$  is the solar constant = 1258.2 W m<sup>-2</sup>

$d_r$  is the relative distance Earth-Sun

$\omega$  is the sunset hour angle (radians)

$\varphi$  is the latitude (radians)

$\delta$  solar declination (radians)

All computations follow:

<http://www.esrl.noaa.gov/gmd/grad/solcalc/calcdetails.html>

```

1      !
2      !-----
3      ! External radiation function
4      !-----
5      !
6      FUNCTION R_extJD(jd,lat)
7      IMPLICIT NONE
8
9      INTEGER, INTENT(IN) :: jd
10     REAL(kind=4), INTENT(IN) :: lat
11
12     REAL(kind=4) :: R_extJD
13
14     Real(kind=4) :: pi
15
16     REAL(kind=4) :: decl, declination, sunr
17     REAL(kind=4) :: daylength, sunrise, sunset
18     REAL(kind=4) :: HDlength, Omega_s, phi_rad, d_r
19
20     pi = 4 * atan(1.)
21
22     decl = (2.*pi/360.) * declination(jd)
23
24     CALL daylen(lat,jd,daylength)
25
26     HDlength=daylength/2.
27     Omega_s=HDlength*pi/12.

```

```

28   phi_rad=lat*(2.*pi/360.)
29   d_r = sunr(jd)
30
31   R_extJD=((1358.2 * (Omega_s * sin(phi_rad) * sin(decl) + cos(phi_rad) * cos(decl) *
sin(Omega_s))) / (pi * d_r**2))
32
33   ! flux_toa_0 = 1358.2 in DSSF, previously 1375. const solar
34
35   END FUNCTION R_extJD
36   !
37   !-----
38   ! Declination function
39   !-----
40   !
41   !
42   FUNCTION declination(jd)
43   IMPLICIT NONE
44
45   INTEGER, INTENT(IN) :: jd
46
47   REAL(kind=4) :: declination
48
49   REAL(kind=4) :: jdc, sec, e0, oblcorr, l0, gmas, seqcent, suntl, sal, delta
50
51   Real(kind=4) :: pi
52
53   pi = 4 * atan(1.)
54
55   jdc=(jd - 2451545.0)/36525.0
56   sec = 21.448 - jdc*(46.8150 + jdc*(0.00059 - jdc*(0.001813)))
57   e0 = 23.0 + (26.0 + (sec/60.0))/60.0
58   oblcorr = e0 + 0.00256 * cos((2.*pi/360.)*(125.04 - 1934.136 * jdc))
59   l0 = 280.46646 + jdc * (36000.76983 + jdc*(0.0003032))
60   l0 = mod(l0-360*(int(l0)/360),360.)
61   gmas = (2.*pi/360.) * (357.52911 + jdc * (35999.05029 - 0.0001537 * jdc))
62   seqcent = sin(gmas) * (1.914602 - jdc * (0.004817 + 0.000014 * jdc)) + &
63   & sin(2.*gmas) * (0.019993 - 0.000101 * jdc) + sin(3.*gmas) * 0.000289
64   suntl = l0 + seqcent
65   sal = suntl - 0.00569 - 0.00478 * sin((2.*pi/360.)*(125.04 - 1934.136 * jdc))
66   delta = asin( sin((2.*pi/360.)*(oblcorr))*sin((2.*pi/360.)*(sal)) )
67
68
69
70
71   declination = (360./(2.*pi)) * delta
72
73   END FUNCTION declination
74   !
75   !-----
76   ! eqtime function
77   !-----
78   !
79   FUNCTION eqtime(jd)
80   IMPLICIT NONE
81
82   INTEGER, INTENT(IN) :: jd

```

```

83
84     REAL(kind=4) :: eqtime
85
86     REAL(kind=4) :: jdc, sec, e0, ecc, oblcorr, y, l0, r0, gmas
87
88     Real(kind=4) :: pi
89
90     pi = 4 * atan(1.)
91
92     jdc=(jd - 2451545.0)/36525.0
93     sec = 21.448 - jdc*(46.8150 + jdc*(0.00059 - jdc*(0.001813)))
94     e0 = 23.0 + (26.0 + (sec/60.0))/60.0
95     ecc = 0.016708634 - jdc * (0.000042037 + 0.0000001267 * jdc)
96     oblcorr = e0 + 0.00256 * cos((2.*pi/360.)*(125.04 - 1934.136 * jdc))
97     y = (tan(((2.*pi/360.)*(oblcorr))/2))**2
98     l0 = 280.46646 + jdc * (36000.76983 + jdc*(0.0003032))
99     l0 = mod(l0-360*(int(l0)/360),360.)
100    r0 = (2.*pi/360.)*(l0)
101    gmas = (2.*pi/360.) * (357.52911 + jdc * (35999.05029 - 0.0001537 * jdc))
102
103    eqtime = y * sin(2.*r0) - 2.0 * ecc * sin(gmas) + 4.0 * ecc * y * sin(gmas) * &
104            & cos(2.*r0) - 0.5 * y**2 * sin(4.*r0) - 1.25 * ecc**2 * sin(2.*gmas)
105    eqtime = 4. * ((360./(2.*pi)) * eqtime)
106
107    END FUNCTION eqtime
108    !
109    !-----
110    ! Sunr function
111    !-----
112    !
113    FUNCTION sunr(jd)
114    IMPLICIT NONE
115
116    INTEGER, INTENT(IN) :: jd
117
118    REAL(kind=4) :: sunr
119
120    REAL(kind=4) :: jdc, ecc, gmas, gmasr, seqc, sta
121
122    Real(kind=4) :: pi
123
124    pi = 4 * atan(1.)
125
126    jdc=(jd - 2451545.0)/36525.0
127    ecc = 0.016708634 - jdc * (0.000042037 + 0.0000001267 * jdc)
128    gmas = 357.52911 + jdc * (35999.05029 - 0.0001537 * jdc)
129    gmasr = (2.*pi/360.) * (gmas)
130    seqc = sin(gmasr) * (1.914602 - jdc * (0.004817 + 0.000014 * jdc)) + &
131            sin(2*gmasr) * (0.019993 - 0.000101 * jdc) + sin(3*gmasr) * 0.000289
132    sta = gmas + seqc
133
134    sunr=(1.000001018 * (1. - ecc**2)) / (1. + ecc * cos((2.*pi/360.)*(sta)))
135
136    END FUNCTION sunr

```

```

137  !
138  !-----
139  ! daylength function
140  !-----
141  !
142  SUBROUTINE daylen(lat,jd,daylength)
143  IMPLICIT NONE
144
145  INTEGER, INTENT(IN) :: jd
146  REAL(kind=4), INTENT(IN) :: lat
147
148  REAL(kind=4) :: daylength
149
150  REAL(kind=4) :: EqTime_1, delta, tanlatdel, omega
151
152  REAL(kind=4) :: eqtime, declination
153
154  Real(kind=4) :: pi
155
156  pi = 4 * atan(1.)
157
158  EqTime_1 = eqtime(jd)
159  delta = declination(jd)
160  tanlatdel = -tan((2.*pi/360.)*(lat)) * tan((2.*pi/360.)*(delta))
161  IF (tanlatdel >1) tanlatdel=1.
162  omega = acos(tanlatdel)
163  daylength = (2.*omega)/(2.*pi/24.)
164  !deltaLatTime = lon
165  !deltaLatTime = deltaLatTime * 24./360.
166  !sunrise = 12. * (1.-omega/pi) - deltaLatTime - EqTime_1/60.
167  !sunset = 12. * (1.+omega/pi) - deltaLatTime - EqTime_1/60.
168
169  !missing_value = -8000
170
171  !IF (omega==0) THEN
172  ! sunrise = missing_value
173  ! sunset = missing_value
174  !END IF
175
176  END SUBROUTINE daylen

```